ANTIOXIDANTS & REDOX SIGNALING
Volume 9, Number 7, 2007
© Mary Ann Liebert, Inc.
DOI: 10.1089/ars.2007.1590

Forum Original Research Communication

Angiotensin II Type 1 Receptor Antagonism Mediates Uncoupling Protein 2-Driven Oxidative Stress and Ameliorates Pancreatic Islet β-Cell Function in Young Type 2 Diabetic Mice

KWAN YI CHU and PO SING LEUNG

ABSTRACT

We recently identified a local pancreatic islet renin-angiotensin system (RAS), and demonstrated that it is upregulated in an animal model of obesity-induced type 2 diabetes mellitus (T2DM). Moreover, angiotensin II type 1 receptor (AT1R) antagonism improves β-cell function and glucose tolerance in young T2DM mice and delays the onset of diabetes. Meanwhile, obesity-induced T2DM results in oxidative stress–mediated activation of uncoupling protein 2 (UCP2), a negative regulator of islet function. In the present study, we postulated that some of the protective effects of AT1R antagonism might be mediated through interference with this pathway and tested this hypothesis in a T2DM animal model. Losartan, an AT1R antagonist, was given to 4-week-old obese *db/db* mice for a period of 8 weeks. UCP2-driven oxidative damage and apoptosis were then analyzed in isolated islets. Losartan selectively inhibited oxidative stress via downregulation of NADPH oxidase; this in turn suppressed UCP2 expression, thus improving β-cell insulin secretion and decreasing apoptosis-induced β-cell mass loss in *db/db* mouse islets. These data indicate that islet AT1R activation in young diabetic mice can generate progressive islet β-cell failure through UCP-driven oxidative damage. *Antioxid. Redox Signal.* 9, 869–878.

GIVEN THAT TYPE 2 diabetes mellitus (T2DM) accounts for >90% of cases of diabetes and its financial drain on healthcare resources, we are in great need of alternative approaches to its prevention and treatment. Between 60% and 90% of T2DM cases appear to be associated with obesity (1). In this context, obesity-associated increased insulin resistance and progressive pancreatic β-cell failure can be considered a key process in the development of T2DM (28, 31). Nevertheless, it is increasingly being recognized that T2DM develops in insulin-resistant subjects only after the onset of β-cell dysfunction. In view of this, continued dysfunction of the β cells and loss of β-cell mass contribute to disease progression (4) and, as such, represent novel therapeutic targets. In this regard, antihypertensive treatment via pharmacologic blockade of the renin–angiotensin system (RAS) may delay or protect (or both) against the development of T2DM in high-risk patients with hypertension (35). The therapeutic benefits of systemic RAS blockade in T2DM prevention and treatment may depend primarily on inhibition of a recently identified local pancreatic islet RAS (19). This local islet RAS plays a key role in pancreatic physiology through the angiotensin II type 1 receptor (AT1R); it regulates pancreatic islet (pro)insulin biosynthesis and local blood flow, and thus glucose-stimulated insulin secretion (5, 18).

The local pancreatic RAS may also play a role in pancreatic *patho*physiology and its treatment: it has been shown to be upregulated in an animal model of obesity-induced T2DM, whereas treatment with the AT1R antagonist losartan can improve β-cell function and glucose tolerance, partly due to enhanced islet (pro)insulin biosynthesis and blood flow (8). In addition, blockade of the islet RAS has been shown to benefit β-cell structure and function, probably through a decrease in islet fibrosis, apoptosis, and oxidative stress (38). Notwithstanding the involvement of an islet RAS in T2DM, how such protective effects are mediated remains to be elucidated.

Department of Physiology, Faculty of Medicine, The Chinese University of Hong Kong, Shatin, Hong Kong, China.

NADPH oxidase is a major source of reactive oxygen species (ROS), which impair β-cell structure and function in T2DM (11, 13, 32, 33). RAS-mediated ROS production may thus play a role in promoting β-cell failure in the diabetic pancreas. The observation that AT1R antagonism decreases oxidative stress by reducing NADPH oxidase activity in pancreatic acinar cells provides strong support for this hypothesis (39). Meanwhile, uncoupling protein 2 (UCP2), a regulator of ROS generation, is upregulated in obesity-induced diabetic animal models and thus has been directly implicated in islet dysfunction and T2DM (6, 7, 26, 41). Such UCP2-induced oxidative damage would be physiologically significant in pancreatic β cells because of their low antioxidant reserve (12, 37). Paradoxically, enhanced UCP2 expression can be protective against oxidative damage and apoptosis in other cell types (3, 9).

In light of these previous findings, we hypothesize that the protective effects of AT1R antagonism may be mediated through a diminution of NADPH oxidase–induced oxidative stress that results in reduced UCP2-mediated islet β-cell dysfunction and apoptosis. We tested this hypothesis in young *db/db* mice, which develop progressive β-cell destruction associated with obesity that arises in the early weeks of life and ultimately develop full-blown T2DM.

MATERIALS AND METHODS

Animal model of T2DM

Genetically diabetic C57BL/KSJ +db/+db (*db/db*) mice and their age-matched nondiabetic littermates C57BL/KSJ m+/+db (*m+/db*) were used for the experiments. The animals were obtained from the Laboratory Animal Services Centre of the Chinese University of Hong Kong. The experimental procedures were approved by the Animal Experimentation Ethics Committee of the Chinese University of Hong Kong (Ref. No. 05/031/ERG).

Prolonged treatment with losartan

Four-week-old obese *db/db* mice were randomly assigned to groups: treated *db/db* mice or nontreated *db/db* mice. The treated *db/db* mice then received losartan (10 mg/kg/day) dissolved in drinking water for 8 weeks, of which the concentration was selected based on our previous study (8). Nontreated *db/db* mice received only plain drinking water, and the age-matched control mice (*m+/db* mice) received drinking water only as the normal control group. An additional group of *m+/db* mice were given the losartan treatment.

Pancreatic islet isolation

Pancreatic islets were isolated as described previously (18). In brief, treated or nontreated *db/db* and the control *m+/db* mice were killed at 12 weeks of age, and the pancreata were dissected out. The pancreata were then placed in cold Hanks' solution (HS) (Sigma Aldrich, St. Louis, MO) and were cut into small pieces of ~1 mm^3. These pieces were transferred to vials containing collagenase solution (Roche Molecular Biochemicals, Mannheim, Germany) and allowed to digest for 6 min. The digest was then washed 3 times by filling the vial with HS. The islets were then examined under a light microscope.

Immunohistochemistry

Pancreas specimens were fixed in 4% (vol/vol) chilled paraformaldehyde and embedded in paraffin. Sections (5 μm thick) were mounted on glass slides, deparaffinized, and processed for indirect immunofluorescent double labeling or immunoperoxidase staining (8, 18). For immunofluorescent labeling, it was used to determine the specific localization of the NADPH oxidase subunit $p22^{phox}$ and the oxidative stress marker nitrotyrosine in islets. Each section was incubated with 4% (wt/vol) normal donkey serum (Jackson ImmunoResearch, West Grove, PA) for 1 h at 37°C to block nonspecific antibody binding. Sections were then incubated overnight at 4°C with anti-$p22^{phox}$ rabbit polyclonal antibody (1:100) (Santa Cruz Biotech, Santa Cruz, CA) or anti-nitrotyrosine mouse monoclonal antibody (1:100) (Zymed, San Francisco, CA) together with anti-insulin goat polyclonal antibody (1:100) (Santa Cruz Biotech). After three washes with phosphate-buffered saline (PBS), the primary antibodies were detected by using a Cy3-conjugated anti-rabbit antibody ($p22^{phox}$) or a Cy3-conjugated anti-mouse antibody (nitrotyrosine), and a FITC-conjugated anti-goat antibody (insulin) (Jackson ImmunoResearch) at room temperature for 1 h. Omission of primary antibodies was used as negative controls. $p22^{phox}$ (red), nitrotyrosine (red), and insulin (green) immunolabeling were detected with a fluorescent microscope equipped with a DC 200 digital camera (Leica Microsystems). β-Cell mass measurements were done in sections incubated with anti-insulin rabbit primary antibody (1:100) (Santa Cruz Biotech) and AMCA-conjugated anti-rabbit secondary antibody (Jackson ImmunoResearch). At least 10 islets per mouse pancreas and five mice per group were randomly chosen for analysis. Islet β-cell mass was assessed by determining the proportion of area occupied by blue fluorescence within each islet (40× objective) using Leica Qwin image-analysis software (Leica Microsystem), as described previously (8).

For immunoperoxidase staining, the ABC staining technique was applied to illustrate the specific localization of UCP2 in the islet cells. Tissue sections were incubated in 0.3% H_2O_2 for 15 min to quench endogenous peroxidase activity and then submerged in 4% (wt/vol) normal donkey serum for 1 h at room temperature to block nonspecific binding. Excess blocking solution was poured off, and the section was incubated overnight at 4°C with anti-UCP2 rabbit polyclonal antibody (1:100) (Alpha Diagnostic, San Antonio, TX) or anti-insulin rabbit polyclonal antibody (1:100) (Santa Cruz Biotech). After three washes with PBS, the primary antibodies were detected with the biotinylated secondary antibody from the Vectastain *Elite* ABC Kit (rabbit IgG) (Vector Laboratories, Burlingame, CA) at room temperature for 1 h. After another three washes with PBS, the sections were incubated with the Vectastain *Elite* ABC Reagent for 1 h at room temperature. The sections were than washed 3 times in PBS and incubated in peroxidase substrate solution (Vector Laboratories) for 2 min for brown color development. After rinsing in nanopure water, sections were counterstained with hematoxylin. The positive brown staining was detected under a light microscope equipped with a DC 200 digital camera (Leica Microsystems).

Real-time RT-PCR analysis

Real-time quantitative reverse transcriptase polymerase chain reaction (RT-PCR) was performed by using an ABI PRISM 7700 Sequence Detection System (PE Applied Biosystems, Foster City, CA), as described previously (8, 18). In brief, total RNA was extracted from pooled islets extracted from control or T2DM mice (groups of eight to 10 mice) by using the Absolutely RNA Microprep Kit (Stratagene, Kirkland, WA) according to the manufacturer's instructions. Total RNA was used as the template in one-step TaqMan amplification reactions. TaqMan primers and probes for $p22^{phox}$, $p67^{phox}$, and UCP2 were designed from mouse cDNA sequence by using Primer Express Software purchased from Applied Biosystems Perkin-Elmer. The primers and probes used were as follows: $p22^{phox}$, 5′-TGGACGTTTCA-CACAGTGGTATT-3′ (sense/forward primer), 5′-TGGACCCCTTTTTCCTCTTTC-3′ (antisense/ reverse primer) and FAM-CCTACTCTATCGCTGCAGGTGTGCTCATC-TAMRA (TaqMan probe); $p67^{phox}$, 5′-CGCTCTCGCCAGAACACA-3′ (sense/forward primer), 5′-AGAGTCAGCAGTAGTTTTTCACTTG-3′ (antisense/ reverse primer) and FAM-TAAACTGAGCTACCGGCGTCGGGA-TAMRA (TaqMan probe); UCP2, 5′-GCATTG-CAGATCTCATCACTTTCC-3′ (sense/forward primer), 5′-AGCCCTTGACTCTCCCCTTG-3′ (antisense/reverse primer), and FAM-TCTGGATACCGCCAAGGTCCGGCT-TAMRA (TaqMan Probe). 18S rRNA was used as an internal control. TaqMan reactions were set up in a reaction volume of 25 μl with TaqMan PCR reagents. Each reaction consisted of 12.5 μl PCR master mix, 0.3 μ*M* of each amplification primer, 0.2 μ*M* corresponding TaqMan probe, and 30 ng RNA template. Each sample was run in duplicate with an initial 30-min period at 48°C and a 10-min period at 95°C to enable reverse transcription, followed by 40 cycles at 95°C for 15 sec and a final 60°C step for 1 min. Amplification data were collected by the 7700 Sequence Detector and analyzed with Sequence Detection System software. The RNA concentration was determined from the threshold cycle (C_T) at which fluorescence was first detected, the cycle number being inversely related to RNA concentration. The fold changes in $p22^{phox}$, $p67^{phox}$, and UCP2 in *db/db* islets were calculated by using the $2^{-\Delta\Delta CT}$ method, as described in the statistical data-analysis section.

Western blot analysis

Islets were isolated from control, treated diabetic, or nontreated diabetic mice and processed for Western blotting, as described previously (8, 18). Total protein of 300 islets was extracted by using the CytoBuster Protein Extraction Reagent (Novagen, Darmstadt, Germany). The protein content of the lysates was determined by a Bio-Rad protein-assay kit (Bio-Rad, Munich, Germany). Western blot analysis of UCP2 was performed. In brief, proteins (10 μg/lane) were subjected to electrophoresis on 12% (wt/vol) polyacrylamide gels. The blotted protein was saturated with 5% (wt/vol) skimmed milk in PBS (pH 7.4) and 0.1% (vol/vol) of Tween 20 for 1 h at room temperature. The membrane was sequentially incubated in rabbit anti-UCP2 antibody (1:1,000) (Alpha Diagnostic, San Antonio, TX) or rabbit anti-caspase 3 antibody (1:1,000) (Santa Cruz Biotech), overnight at 4°C and a peroxidase-labeled anti-rabbit IgG antibody (1:1,500) (Amersham, Little Chalfont Buckinghamshire, UK) for 1 h at room temperature. Labeled protein bands were revealed by application of ECL Plus Western blotting detection reagents and autoradiography film (Amersham). The chemiluminescence intensity of the bands was quantified by using an image analyzer (Molecular Dynamics Image Quant, Sunnyvale, CA).

Measurement of islet apoptosis

Islet cell death was assessed by the Cell Death Detection ELISAplus assay (Roche) according to the procedures recommended by the manufacturer (23). One hundred islets of comparable size were incubated for 30 min with a lysis buffer at room temperature and then centrifuged at 200 *g* for 10 min at 4°C. Aliquots of the supernatant (20 μl) were placed into streptavidin-coated microtiter plate wells, and 80-μl aliquots of a mixture containing anti-histone-biotin and anti-DNA-POD antibodies were then added and incubated for 2 h at room temperature. The preparations were then washed, and 200 μl of a solution containing ABTS (the substrate for POD) was added. At the end of a 15-min incubation, absorbance of samples was read spectrophotometrically at 405 nm.

Measurements of islet insulin release

Islet insulin release was measured by enzyme-link immunosorbent assay (ELISA) in groups of 10, as described previously (8, 18). In brief, samples were transferred in duplicate to Falcon 24-well culture plates containing 0.25 ml Krebs-Ringer bicarbonate buffer (KRBB) supplemented with 10 m*M* HEPES and 2 mg/ml of bovine serum albumin (BSA). Islets were incubated for 1 h at 37°C (O_2/CO_2, 95:5) in medium containing 1.7 m*M* glucose, and then incubated for an additional hour in 0.25 ml of KRBB containing 16.7 m*M* glucose. After the incubation, media were collected for measurement of insulin release by using a Mouse Insulin ELISA Kit (Mercodia, Uppsala, Sweden).

Statistical data analysis

Results are expressed as means ± standard errors (SEM) for all groups. Multiple comparisons between groups were performed by using an analysis of variance (ANOVA) followed by Tukey's *post hoc* test, or, when comparisons were made only relative to controls, by Dunnett's test. When only two groups were compared, probabilities (p) of chance differences between the experimental groups were calculated with student's unpaired two-tailed t test. For all comparisons, $p < 0.05$ was considered statistically significant. For real-time RT-PCR, relative expression was normalized as a percentage of 18S rRNA and calculated by using the comparative C_T method of $2^{-\Delta\Delta CT}$, as described previously (8, 18).

RESULTS

Effects of losartan on oxidative stress production

Blood glucose levels of the *m+/db* mice were unaffected by losartan when compared with those in the nontreated *m+/db* mice, as evidenced by previous and present studies (data not shown); thus, the losartan-treated *m+/db* group was eliminated

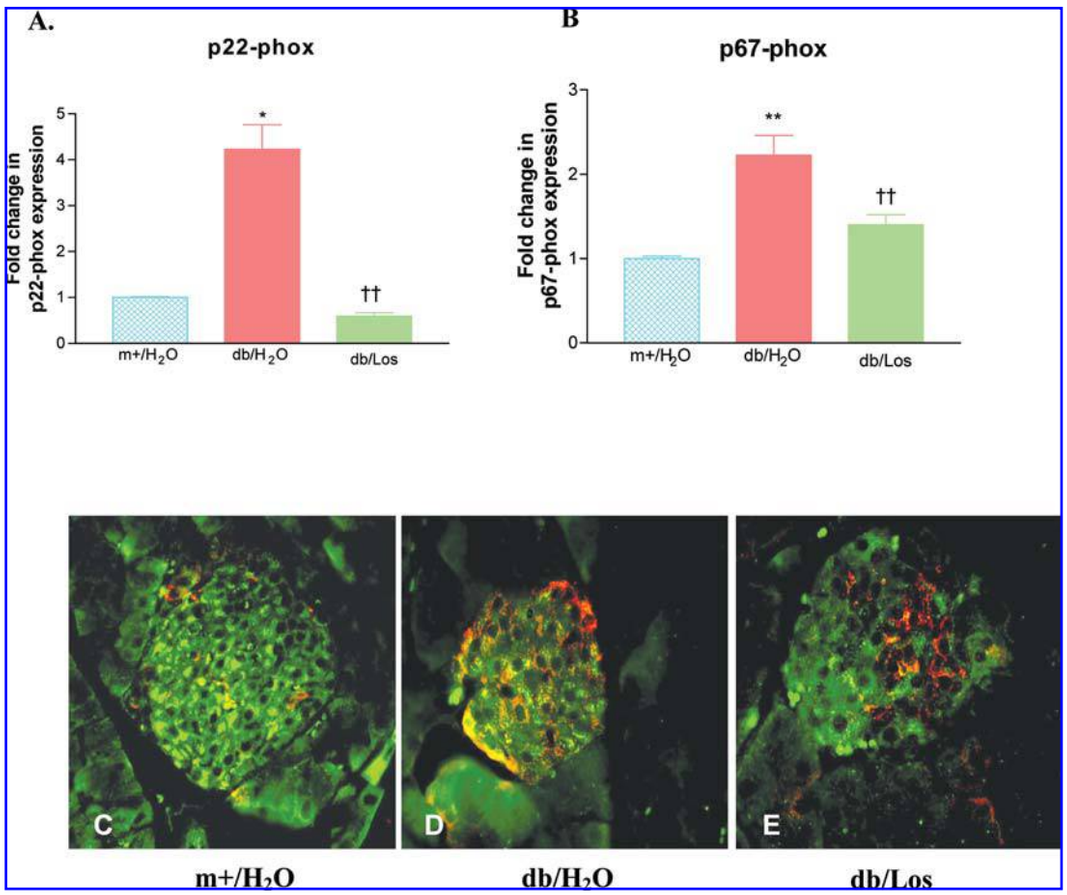

FIG. 1. Expression of NADPH oxidase subunits, $p22^{phox}$ and $p67^{phox}$. (**A, B**) Relative mRNA expression levels of $p22^{phox}$ and $p67^{phox}$ in control ($m+/H_2O$), diabetic (db/H_2O), and losartan-treated diabetic mice (db/Los). (**C**–**E**) Double-immunofluorescent localization of $p22^{phox}$ (red) and insulin (green) in the mouse pancreatic islets. Relative expression was normalized as a percentage of 18S rRNA calculated by using the comparative C_T method of $2^{-\Delta\Delta CT}$. All data are expressed as mean ± SEM ($n = 6$). *$p < 0.05$, **$p < 0.01$ vs. $m+/H_2O$. ††$p < 0.01$ vs. db/H_2O mice. (For interpretation of the references to color in this figure legend, the reader is referred to the web version of this article at www.liebertonline.com/ars)

for subsequent experiments in this study. Real-time PCR and double immunolabeling were applied to determine the NADPH oxidase level in the islets (Fig. 1). The PCR experiments revealed that that mRNA expression of the NADPH oxidase subunits $p22^{phox}$ and $p67^{phox}$ were increased fourfold and twofold, respectively, in the nontreated *db/db* mice islet ($p22^{phox}$: 4.23 ± 0.53; $p67^{phox}$: 2.23 ± 0.24; $n = 5$) relative to normal control mice ($p22^{phox}$: 1.00 ± 0.01; $p67^{phox}$: 1.00 ± 0.03; $p < 0.01$; $n = 5$). Meanwhile, 8-week losartan treatment (10 mg/kg/day) suppressed NADPH oxidase subunit mRNA expression relative to that of the nontreated *db/db* mice ($p22^{phox}$: 0.60 ± 0.07; $p < 0.001$; $p67^{phox}$: 1.40 ± 0.12; $p < 0.01$; $n = 6$) (Fig. 1A and B). The double immunofluorescent labeling results were consistent with the real-time PCR findings. Basal expression of $p22^{phox}$ (red) in the normal islet in different cell types, including pancreatic (cells, is shown in Fig. 1C. In the nontreated *db/db* mouse islets, $p22^{phox}$ was highly upregulated, and a larger proportion of β cells was positively labeled with the $p22^{phox}$ (Fig. 1D). Although losartan treatment could not reduce $p22^{phox}$ expression back to basal level (Fig. 1C), losartan significantly reduced the number of $p22^{phox}$ immunoreactive cells compared with nontreated islets (Fig. 1D) and essentially all of the remaining labeled cells were non-β cells (Fig. 1E).

To confirm the oxidative stress level in the islets, nitrotyrosine, the oxidative stress marker commonly used previously (2, 22, 38), was detected by double immunofluorescent labeling. Whereas little positive nitrotyrosine labeling (red) could be seen in normal control islets (Fig. 2A), nitrotyrosine labeling was obviously increased in both β cells and non–β cells in the nontreated *db/db* mice (Fig. 2B). Again, losartan effectively reduced the oxidative stress level, as evidenced by the reduction in nitrotyrosine immunoreactivity (Fig. 2C).

Effects of losartan on UCP2 expression

The UCP2 expression levels in the pancreatic islets of all groups of mice are shown in Fig. 3. Real-time quantitative RT-PCR analysis (Fig. 3A) revealed that the mean UCP2 mRNA level in the nontreated *db/db* mouse islets (5.01 ± 0.59; $p < 0.0001$; $n = 13$) was about fivefold higher than that of the normal control (1.00 ± 0.01; $n = 3$). RAS blockade with losartan downregulated UCP2 mRNA expression in *db/db*

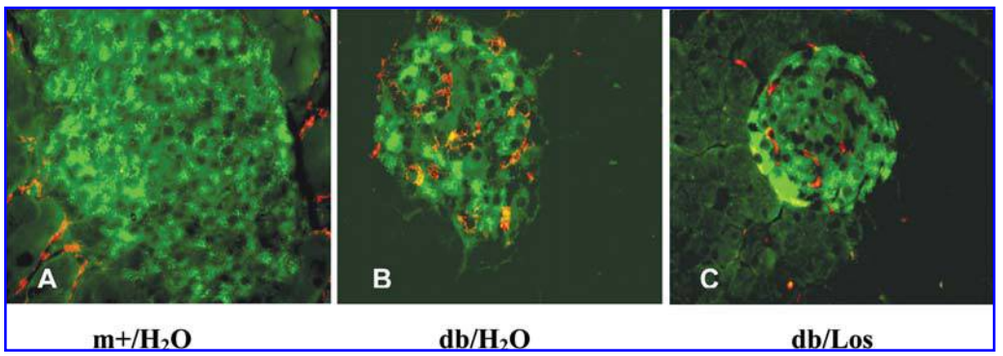

FIG. 2. Immunohistochemical localization of nitrotyrosine (red) and insulin (green) in (A) control (m+/H_2O), (B) diabetic (db/H_2O), and (C) losartan-treated diabetic (db/Los) mouse pancreatic islets. (For interpretation of the references to color in this figure legend, the reader is referred to the web version of this article at www.liebertonline.com/ars)

mouse islets by ~50% (2.44 ± 0.31; $p < 0.05$; $n = 10$). Immunoperoxidase staining was performed to validate further the presence and expression levels of UCP2 in the islets of the different groups of mice. The normal control mice ($n = 4$) showed a positive light-brown color throughout the islets, which served as a reference for basal expression of UCP2 (Fig. 3C). Extensive UCP2 staining with greater intensity was observed throughout the islets of *db/db* mice ($n = 5$) (Fig. 3E). However, losartan-treated *db/db* mouse islets ($n = 5$) demonstrated a clear reduction in UPC2 immunoreactive area (Fig. 3G), compared with the nontreated *db/db* mouse islets (Fig. 3E); although some immunoreactivity persisted in the peripheral regions (Fig. 3G). More quantitatively to compare UCP2 expression in losartan-treated and nontreated pancreatic islets, Western blot analysis was carried out (Fig. 3H and I). An ~32-kDA protein, consistent with UCP2, was detected in the mice pancreatic islet samples. Losartan treatment reduced UCP2 protein expression by 50% ($n = 6$) relative to nontreated *db/db* mouse islets ($n = 10$). These results clearly indicated that the islets isolated from losartan-treated *db/db* mice expressed significantly less UCP2 protein than islets isolated from nontreated diabetic mice.

Effects of losartan on apoptosis

The protein expression levels of the apoptotic cell marker caspase 3 were assessed in the islets from losartan-treated and nontreated mice by Western blot analysis (Fig. 4A). Caspase 3 expression was normalized relative to β-actin (Fig. 4B). Whereas normal islets showed a low basal expression of caspase 3, expression of this protein was increased threefold in nontreated diabetic islets. Meanwhile, losartan treatment reduced caspase 3 expression by >50% in diabetic islets. Enzyme-linked immunosorbent assay (ELISA) studies were conducted to substantiate the degree of programmed cell death (Fig. 5). Comparing 100 islets of similar size in each group, the normal control (0.95 ± 0.33; $n = 6$) showed much less apoptosis than the diabetic group (12.72 ± 0.93; $p < 0.001$; $n = 4$). Losartan significantly reduced this level compared with that of the nontreated diabetic group (5.31 ± 1.23; $p < 0.001$; $n = 6$), although a greater level of apoptosis was present than in normal controls. Our fluorescent immunohistochemistry results (Fig. 6) revealed that the major proportions of normal islets were made up of β cells (blue) (Fig. 6A–C). The diabetic islet, however, exhibited a sharply reduced β-cell mass, and this deficit was ameliorated by losartan treatment (Fig. 6D). The various approaches we applied displayed a consistent pattern, indicating that β-cell apoptosis was involved in obesity-induced T2DM and that this apoptosis can be ameliorated by losartan treatment.

Effects of losartan on insulin secretion

β-Cell function was assessed by measuring the insulin secretory ability of the islets (Fig. 7). Although all groups of islets responded to the high-glucose challenge, the diabetic group exhibited the lowest magnitude of the insulin response to high-glucose stimulation (1.13 ± 0.42 μg/islet/h; $p < 0.001$; $n = 5$). Meanwhile, the normal control and the losartan-treated groups demonstrated much greater responses (4.1 ± 0.56 and 3.45 ± 0.65 μg/islet/h respectively; $p < 0.05$ for losartan-treated group; $n = 5$). Thus, AT1R blockade appears to improve effectively the glucose-stimulated insulin secretion in the diabetic mice.

DISCUSSION

Apart from its hemodynamic action, the RAS has multiple cellular roles influencing, for instance, proliferation, apoptosis, and ROS formation at the levels of tissues and organs (27). Of great interest in this context is the recently identified pancreatic islet RAS, which may have novel roles in islet function and diabetes (19). In the *in vitro* studies of acute RAS, blockade has been shown to exert positive effects on islet (pro)insulin biosynthesis and glucose-stimulated insulin secretion in isolated pancreatic islets (18, 22). Meanwhile, other studies have found that briefly exposing isolated islets to angiotensin II can cause a rapid and transient surge in insulin secretion through a calcium-mediated regulatory mechanism (30). We have recently shown that pancreatic islet RAS is upregulated in obese *db/db* mice. Moreover, we demonstrated in an *in vivo* study that chronic AT1R blockade in 4-week-old *db/db* mice for an 8-week period improved β-cell function and glucose tolerance, and that these effects results in a delay in the onset of T2DM in these young diabetic mice; some of these protective effects

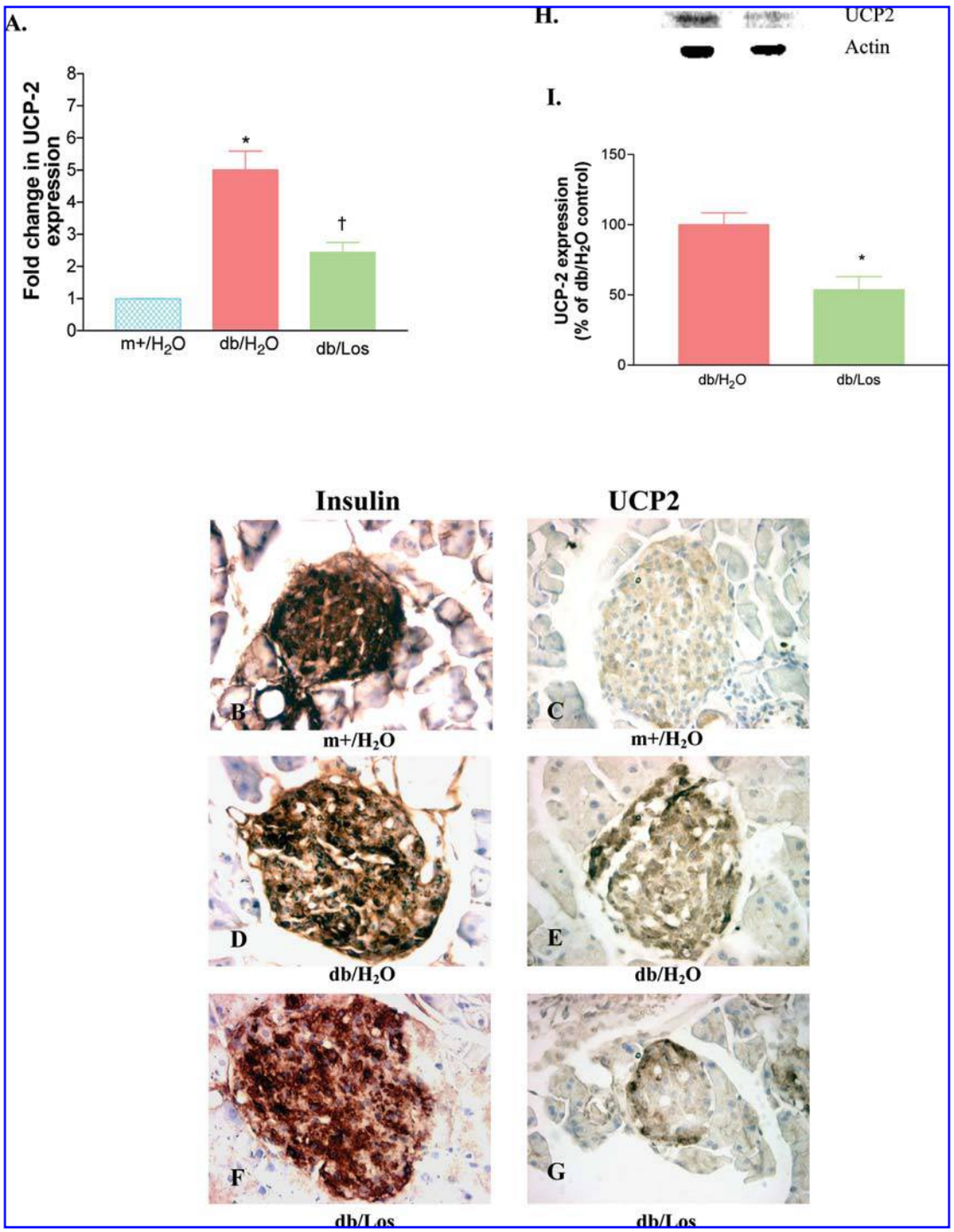

FIG. 3. Expression of UCP-2. (**A**) Relative mRNA expression level was normalized as a percentage of 18S rRNA calculated by using the comparative C_T method of $2^{-\Delta\Delta CT}$. (**B–G**) Immunoperoxidase localization, and (**H**) protein expression level of UCP-2 in control (m+/H_2O), diabetic (db/H_2O), and losartan-treated diabetic mice (db/Los). (**I**) The relative expression was normalized as a percentage of the actin signal. All data are expressed as mean ± SEM ($n = 6$). $^{**}p < 0.01$ vs. m+/H_2O. $^{\dagger\dagger}p < 0.01$ vs. db/H_2O mice. (For interpretation of the references to color in this figure legend, the reader is referred to the web version of this article at www.liebertonline.com/ars)

were attributable to AT1R-mediated alterations in islet (pro)insulin biosynthesis and blood flow (8). Consistent with our findings, Tikellis *et al.* (38) showed that chronic (10 weeks) RAS inhibition starting at the age of 10 weeks attenuated disordered islet architecture in Zucker diabetic fatty (ZDF) rats; these beneficial effects were partly attributed to increased intraislet fibrosis, apoptosis, and oxidative stress (38). However, RAS inhibition did not influence long-term

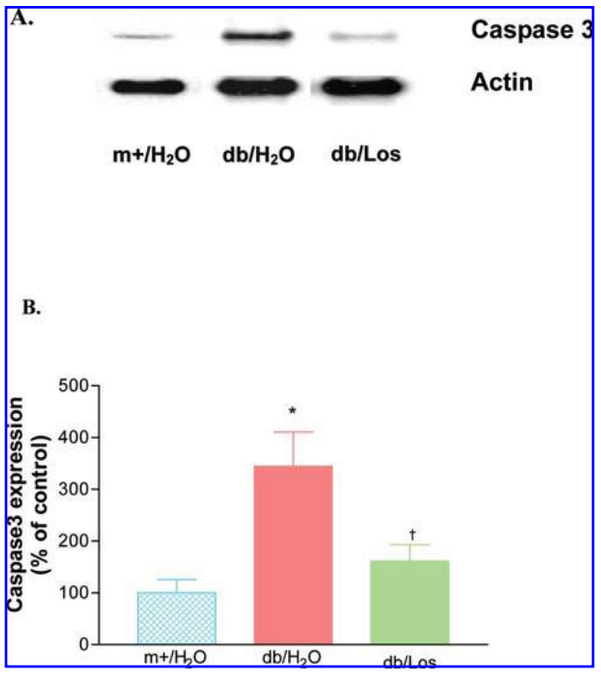

FIG. 4. Protein expression of caspase 3. (**A**) Western blot analysis of actin and caspase 3. (**B**) The relative expression was normalized as a percentage of the actin signal. All data are expressed as mean ± SEM ($n = 5$). *$P < 0.05$ vs. m+ control. (For interpretation of the references to color in this figure legend, the reader is referred to the web version of this article at www.liebertonline.com/ars)

glycemic control or protect against the onset of diabetes in the ZDF animal model.

In the present study, we focused on AT1R activation–mediated NADPH oxidase–dependent generation of ROS and its interaction with UCP2 in the regulation of pancreatic β-cell function and apoptosis. In fact, angiotensin II is well known to stimulate the PKC–NADPH oxidase pathway, thus initiating ROS production in cardiomyocytes and vascular smooth muscle cells (15, 42). However, the signaling pathway(s) in the pancreatic β cell triggered by angiotensin II

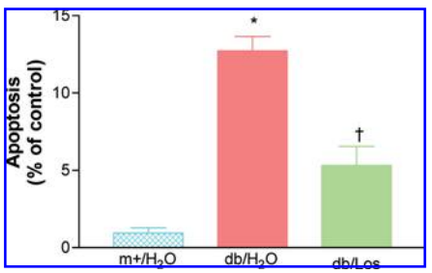

FIG. 5. Apoptotic level in islets from nontreated diabetic, treated diabetic, and control mice. All data are expressed as mean ± SEM ($n = 5$). *$p < 0.05$ vs. m+ control. (For interpretation of the references to color in this figure legend, the reader is referred to the web version of this article at www.liebertonline.com/ars)

through AT1R remain to be elucidated. In this study, we found that an earlier AT1R intervention (beginning at 4 weeks of age) selectively inhibited oxidative stress by downregulation of NADPH oxidase; this in turn suppressed UCP2 expression, improved β-cell insulin secretion, and decreased apoptosis-induced β-cell mass loss in these young obese *db/db* mice. RAS activation has been suggested to be a key stimulator of NADPH oxidase, which increases ROS generation within different cell types such as vascular muscle cells (14), pancreatic acinar cells (39) and islet β cells (25). In the present study, and in keeping with recent findings, we verified that chronic AT1R antagonism decreases NADPH oxidase–induced oxidative stress (24, 34). Although activation of NADPH oxidase by the RAS was demonstrated to reduce insulin secretion from islets, the novel involvement of potential mechanistic pathway(s) by which activation of the AT1R–NADPH oxidase–UCP2 pathway achieves oxidative damage have yet to be elucidated. Herein, we have demonstrated that such actions may be mediated, at least in part, through interference in UCP2 expression. Although UCP2 has previously been suggested to be a negative regulator of insulin secretion (7, 41), the present study is the first to report evidence indicating that the local RAS is a potential upstream activator of UCP2 in islets.

The mechanisms of β-cell failure in T2DM are diverse and complicated. The genetic and acquired defects include, but are not limited to, mitochondrial dysfunction, oxidative stress, endoplasmic reticulum stress, dysfunctional triglyceride/free fatty acid cycling, and glucotoxicity, as well as lipotoxicity (29). Among these, mitochondrial dysfunction accompanied with excess ROS production plays a critical role in T2DM (21). In this regard, superoxide-mediated activation of UCP2 by obesity and hyperglycemia causes β-cell dysfunction (16). Hyperlipidemia and hyperglycemia, as observed in T2DM, can induce UCP2 expression in pancreatic β cells (17). UCP2 activation acts to dissipate safely the elevated mitochondrial membrane potential at the expense of ATP synthesis and consequently glucose-stimulated insulin secretion; in other words, uncoupling of oxidative phosphorylation results in impaired insulin secretory capacity while reducing ROS generation (6, 21). Interestingly, UCP2 and its family members can also act as a regulator of oxidative stress, protecting the cell against ROS and preventing glucose-induced apoptosis (20, 40). Thus, suppression of UCP2 could be a detrimental process in provoking β-cell apoptosis, because the β cell is vulnerable to oxidative stress damage owing to its low endogenous antioxidant activity (12, 37).

Although insufficient evidence exists to date to prove a direct RAS–UCP2 interaction, if there were a reduction in UCP2 expression without oxidative stress inhibition after AT1R blockade, we expect that this reduction would probably exert a negative effect on β-cell survival. To examine the validity of this causal relation, we quantified β-cell apoptosis in the present study. β-Cell apoptosis and UCP2 expression were significantly reduced by prolonged losartan treatment, suggesting that a direct action of AT1R agonism on UCP2 expression is not likely. Instead, AT1R could exert its action on UCP2 through NADPH oxidase activation. Thus, two possible mechanisms exist whereby insulin secretion could be enhanced by AT1R blockade: (a) AT1R antagonism may suppress NADPH

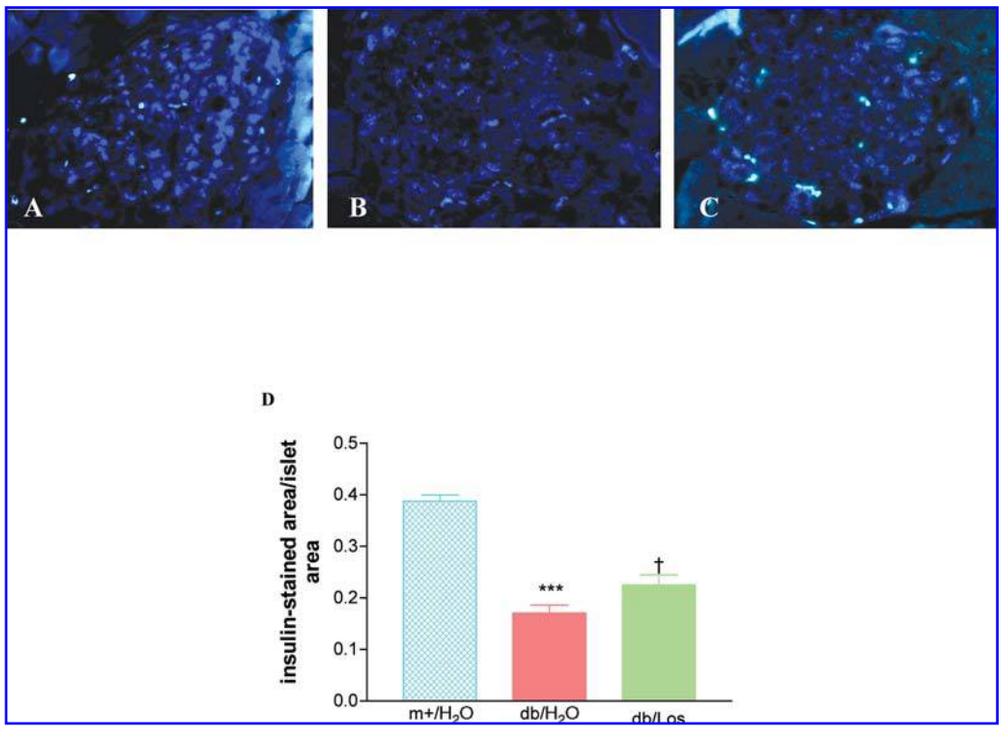

FIG. 6. Effect of losartan on β-cell mass in (A) control (m+/db), (B) nontreated diabetic (db/H_2O), and (C) losartan-treated diabetic (db/Los) mouse islets. Magnification, 40×. Bar, 40 μm. **D**, Relative labeled areas are plotted. Each value represents the mean ± SEM ($n = 11$). ***$p < 0.001$ vs. m+ control. †$p < 0.05$ vs. db/H_2O group. (For interpretation of the references to color in this figure legend, the reader is referred to the web version of this article at www.liebertonline.com/ars)

oxidase, which results in UCP2 reduction and consequently enhances insulin secretion; (b) alternatively, a decrease in NADPH oxidase–induced oxidative stress may rescue β cells from apoptosis, which increases β-cell mass within the islet, and ultimately augments insulin secretion.

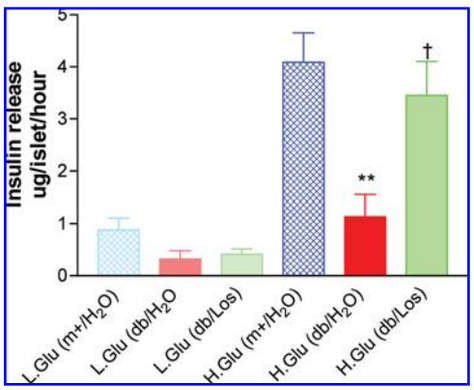

FIG. 7. Comparison of insulin release from control (m+/H_2O), nontreated diabetic (db/H_2O) and treated diabetic (db/Los) mouse islets, in the presence of 1.7 (low; L. Glu) or 16.7 m*M* (high; H. Glu) glucose. **$p < 0.01$ vs. m+/H_2O islets exposed to 16.7 m*M* glucose only. †$p < 0.05$ vs. db/H_2O islets exposed to 16.7 m*M* glucose only. (For interpretation of the references to color in this figure legend, the reader is referred to the web version of this article at www.liebertonline.com/ars)

In the present study, we chose to administer losartan to *db/db* mice starting from the age of 4 weeks, a time when T2DM has not yet fully developed, so that we could better study protection against progression in this disease. Our observations that β-cell apoptosis could not be restored *fully* back to the basal level by the losartan treatment, suggest that AT1R activation is a partial cause of β-cell apoptosis. Whereas several causal factors exist, most of them involved in inflammatory processes, that have implicated in regulating β-cell secretory function and cell turnover (10), the RAS has been known to be a key mediator of inflammation (36). Moreover, we have also shown UCP2 to be

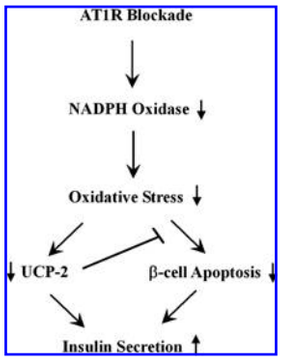

FIG. 8. Proposed pathways for AT1R blockade–mediated oxidative stress and UCP2 axis in on pancreatic β-cell apoptosis and secretion.

a new candidate affected by RAS activation and involved in depressed insulin secretion. Elucidating the role and the downstream mediator(s) or pathway(s) of UCP2 activation in insulin secretion will require further investigation.

In conclusion, the present study in an animal model of obesity-induced diabetes indicates that AT1R antagonism attenuates NADPH oxidase–induced oxidative stress; this in turn results in a downregulation of UCP2 expression, which was associated with improved β-cell insulin secretion and reduced apoptosis-induced β-cell mass loss (see Fig. 8 for a summary). These findings serve as a proof-of-principle investigation, indicating that islet AT1R activation in young diabetic mice mediates progressive islet β-cell failure through UCP-driven oxidative damage.

ACKNOWLEDGMENTS

We gratefully acknowledge support from a Competitive Earmarked Research Grant from the Research Grants Council of Hong Kong (Project no. CUHK4537/05M and CUHK4364/04M), a Direct Grant of Research from the Chinese University of Hong Kong (Project no. 2041158), and the MERCK-COZAAR Medical School Grant Program (Ref. no. 5868), awarded to P.S.L.

ABBREVIATIONS

AT1R, angiotensin II type 1 receptor; RAS, renin–angiotensin system; ROS, reactive oxygen species; T2DM, type 2 diabetes mellitus; UCP2, uncoupling protein 2; ZDF rats, Zucker diabetic fatty rats.

REFERENCES

1. Anderson JW, Kendall CW, and Jenkins DJ. Importance of weight management in type 2 diabetes: review with meta-analysis of clinical studies. *J Am Coll Nutr* 22: 331–339, 2003.
2. Beckman JS and Koppenol WH. Nitric oxide, superoxide, and peroxynitrite: the good, the bad, and ugly. *Am J Physiol* 271: C1424–C1437, 1996.
3. Blanc J, ves-Guerra MC, Esposito B, Rousset S, Gourdy P, Ricquier D, Tedgui A, Miroux B, and Mallat Z. Protective role of uncoupling protein 2 in atherosclerosis. *Circulation* 107: 388–390, 2003.
4. Butler AE, Janson J, Bonner-Weir S, Ritzel R, Rizza RA, and Butler PC. Beta-cell deficit and increased beta-cell apoptosis in humans with type 2 diabetes. *Diabetes* 52 : 102–110, 2003.
5. Carlsson PO, Berne C, and Jansson L. Angiotensin II and the endocrine pancreas: effects on islet blood flow and insulin secretion in rats. *Diabetologia* 41: 127–133, 1998.
6. Chan CB, Saleh MC, Koshkin V, and Wheeler MB. Uncoupling protein 2 and islet function. *Diabetes* 53(suppl 1): S136–S142, 2004.
7. Chan CB, MacDonald PE, Saleh MC, Johns DC, Marban E, and Wheeler MB. Overexpression of uncoupling protein 2 inhibits glucose-stimulated insulin secretion from rat islets. *Diabetes* 48: 1482–1486, 1999.
8. Chu KY, Lau T, Carlsson PO, and Leung PS. Angiotensin II type 1 receptor blockade improves beta-cell function and glucose tolerance in a mouse model of type 2 diabetes. *Diabetes* 55: 367–374, 2006.
9. Collins P, Jones C, Choudhury S, Damelin L, and Hodgson H. Increased expression of uncoupling protein 2 in HepG2 cells attenuates oxidative damage and apoptosis. *Liver Int* 25: 880–887, 2005.
10. Donath MY and Halban PA. Decreased beta-cell mass in diabetes: significance, mechanisms and therapeutic implications. *Diabetologia* 47: 581–589, 2004.
11. Evans JL, Goldfine ID, Maddux BA, and Grodsky GM. Are oxidative stress-activated signaling pathways mediators of insulin resistance and beta-cell dysfunction? *Diabetes* 52: 1–8, 2003.
12. Fridlyand LE and Philipson LH. Does the glucose-dependent insulin secretion mechanism itself cause oxidative stress in pancreatic beta-cells? *Diabetes* 53: 1942–1948, 2004.
13. Green K, Brand MD, and Murphy MP. Prevention of mitochondrial oxidative damage as a therapeutic strategy in diabetes. *Diabetes* 53(suppl 1): S110–S118, 2004.
14. Griendling KK, Minieri CA, and Ollerenshaw JD, Alexander RW. Angiotensin II stimulates NADH and NADPH oxidase activity in cultured vascular smooth muscle cells. *Circ Res* 74: 1141–1148, 1994.
15. Inoguchi T and Nawata H. NAD(P)H oxidase activation: a potential target mechanism for diabetic vascular complications, progressive beta-cell dysfunction and metabolic syndrome. *Curr Drug Targets* 6: 495–501, 2005.
16. Krauss S, Zhang CY, Scorrano L, Dalgaard LT, St-Pierre J, Grey ST, and Lowell BB. Superoxide-mediated activation of uncoupling protein 2 causes pancreatic beta cell dysfunction. *J Clin Invest* 112: 1831–1842, 2003.
17. Lameloise N, Muzzin P, Prentki M, and Assimacopoulos-Jeannet F. Uncoupling protein 2: a possible link between fatty acid excess and impaired glucose-induced insulin secretion? *Diabetes* 50: 803–809, 2001.
18. Lau T, Carlsson PO, and Leung PS. Evidence for a local angiotensin-generating system and dose-dependent inhibition of glucose-stimulated insulin release by angiotensin II in isolated pancreatic islets. *Diabetologia* 47: 240–248, 2004.
19. Leung PS and Carlsson PO. Pancreatic islet renin angiotensin system: its novel roles in islet function and in diabetes mellitus. *Pancreas* 30: 293–298, 2005.
20. Li LX, Skorpen F, Egeberg K, Jorgensen IH, and Grill V. Uncoupling protein-2 participates in cellular defense against oxidative stress in clonal beta-cells. *Biochem Biophys Res Commun* 282: 273–277, 2001.
21. Lowell BB and Shulman GI. Mitochondrial dysfunction and type 2 diabetes. *Science* 307: 384–387, 2005.
22. Lupi R, Del GS, Bugliani M, Boggi U, Mosca F, Torri S, Del PS, and Marchetti P. The direct effects of the angiotensin-converting enzyme inhibitors, zofenoprilat and enalaprilat, on isolated human pancreatic islets. *Eur J Endocrinol* 154: 355–361, 2006.
23. Marselli L, Dotta F, Piro S, Santangelo C, Masini M, Lupi R, Realacci M, del GS, Mosca F, Boggi U, Purrello F, Navalesi R, and Marchetti P. Th2 cytokines have a partial, direct protective effect on the function and survival of isolated human islets exposed to combined proinflammatory and Th1 cytokines. *J Clin Endocrinol Metab* 86: 4974–4978, 2001.
24. Nakayama M, Inoguchi T, Sonta T, Maeda Y, Sasaki S, Sawada F, Tsubouchi H, Sonoda N, Kobayashi K, Sumimoto H, and Nawata H. Increased expression of NAD(P)H oxidase in islets of animal models of type 2 diabetes and its improvement by an AT1 receptor antagonist. *Biochem Biophys Res Commun* 332: 927–933, 2005.
25. Oliveira HR, Verlengia R, Carvalho CR, Britto LR, Curi R, and Carpinelli AR. Pancreatic beta-cells express phagocyte-like NAD(P)H oxidase. *Diabetes* 52: 1457–1463, 2003.
26. O'Rahilly S. Uncoupling protein, 2: adiposity angel and diabetes devil? *Nat Med* 7: 770–772, 2001.
27. Paul M, Poyan MA, and Kreutz R. Physiology of local renin-angiotensin systems. *Physiol Rev* 86: 747–803, 2006.
28. Porte D Jr. Banting lecture 1990: beta-cells in type II diabetes mellitus. *Diabetes* 40: 166–180, 1991.
29. Prentki M and Nolan CJ. Islet beta cell failure in type 2 diabetes. *J Clin Invest* 116: 1802–1812, 2006.
30. Ramracheya RD, Muller DS, Wu Y, Whitehouse BJ, Huang GC, Amiel SA, Karalliedde J, Viberti G, Jones PM, and Persaud SJ. Direct regulation of insulin secretion by angiotensin II in human islets of Langerhans. *Diabetologia* 49: 321–331, 2006.
31. Reaven GM. Banting lecture 1988: Role of insulin resistance in human disease. *Diabetes* 37: 1595–1607, 1988.

32. Sakuraba H, Mizukami H, Yagihashi N, Wada R, Hanyu C, and Yagihashi S. Reduced beta-cell mass and expression of oxidative stress-related DNA damage in the islet of Japanese type II diabetic patients. *Diabetologia* 45: 85–96, 2002.
33. Schrauwen P and Hesselink MK. Oxidative capacity, lipotoxicity, and mitochondrial damage in type 2 diabetes. *Diabetes* 53: 1412–1417, 2004.
34. Shao J, Iwashita N, Ikeda F, Ogihara T, Uchida T, Shimizu T, Uchino H, Hirose T, Kawamori R, and Watada H. Beneficial effects of candesartan, an angiotensin II type 1 receptor blocker, on beta-cell function and morphology in db/db mice. *Biochem Biophys Res Commun* 344: 1224–1233, 2006.
35. Stump CS, Hamilton MT, and Sowers JR. Effect of antihypertensive agents on the development of type 2 diabetes mellitus. *Mayo Clin Proc* 81: 796–806, 2006.
36. Suzuki Y, Ruiz-Ortega M, Lorenzo O, Ruperez M, Esteban V, and Egido J. Inflammation and angiotensin II. *Int J Biochem Cell Biol* 35: 881–900, 2003.
37. Tiedge M, Lortz S, Drinkgern J, and Lenzen S. Relation between antioxidant enzyme gene expression and antioxidative defense status of insulin-producing cells. *Diabetes* 46: 1733–1742, 1997.
38. Tikellis C, Wookey PJ, Candido R, Andrikopoulos S, Thomas MC, and Cooper ME. Improved islet morphology after blockade of the renin- angiotensin system in the ZDF rat. *Diabetes* 53: 989–997, 2004.
39. Tsang SW, Ip SP, and Leung PS. Prophylactic and therapeutic treatments with AT_1 and AT_2 receptor antagonists and their effects on changes in the severity of pancreatitis. *Int J Biochem Cell Biol* 36: 330–339, 2004.
40. Vincent AM, Olzmann JA, Brownlee M, Sivitz WI, and Russell JW. Uncoupling proteins prevent glucose-induced neuronal oxidative stress and programmed cell death. *Diabetes* 53: 726–734, 2004.
41. Zhang CY, Baffy G, Perret P, Krauss S, Peroni O, Grujic D, Hagen T, Vidal-Puig AJ, Boss O, Kim YB, Zheng XX, Wheeler MB, Shulman GI, Chan CB, and Lowell BB. Uncoupling protein-2 negatively regulates insulin secretion and is a major link between obesity, beta cell dysfunction, and type 2 diabetes. *Cell* 105: 745–755, 2001.
42. Zhang Y, Bloem LJ, Yu L, Estridge TB, Iversen PW, McDonald CE, Schrementi JP, Wang X, Vlahos CJ, and Wang J. Protein kinase C beta II activation induces angiotensin converting enzyme expression in neonatal rat cardiomyocytes. *Cardiovasc Res* 57: 139–146, 2003.

Address reprint requests to:
Professor P. S. Leung, Ph.D.
Department of Physiology
Faculty of Medicine
The Chinese University of Hong Kong
Shatin, New Territories, Hong Kong

E-mail: psleung@cuhk.edu.hk

Date of first submission to ARS Central, January 28, 2007; date of acceptance, February 15, 2007.

This article has been cited by:

1. Nynke J. van der Zijl, Chantalle C.M. Moors, Gijs H. Goossens, Ellen E. Blaak, Michaela Diamant. 2012. Does interference with the renin-angiotensin system protect against diabetes? Evidence and mechanisms. *Diabetes, Obesity and Metabolism* no-no. [CrossRef]
2. Yuk Cheung Chan , Po Sing Leung . 2011. The Renin–Angiotensin System and Reactive Oxygen Species: Implications in Pancreatitis. *Antioxidants & Redox Signaling* **15**:10, 2743-2755. [Abstract] [Full Text HTML] [Full Text PDF] [Full Text PDF with Links]
3. Qianni Cheng, Po Sing Leung. 2011. An update on the islet renin–angiotensin system. *Peptides* **32**:5, 1087-1095. [CrossRef]
4. Man Ting Ma, Kwan Keung Leung, Kam Sze Tsang, Po Sing Leung. 2011. Reduced immunogenicity of pancreatic progenitor cells derived from first-trimester human fetal pancreas. *The International Journal of Biochemistry & Cell Biology* **43**:5, 812-820. [CrossRef]
5. Q. Cheng, Y. C. Li, B. J. Boucher, P. S. Leung. 2011. A novel role for vitamin D: modulation of expression and function of the local renin–angiotensin system in mouse pancreatic islets. *Diabetologia* . [CrossRef]
6. Hong-Wei Wang, Masanari Mizuta, Yukie Saitoh, Kenji Noma, Hiroaki Ueno, Masamitsu Nakazato. 2011. Glucagon-like peptide–1 and candesartan additively improve glucolipotoxicity in pancreatic #-cells. *Metabolism* . [CrossRef]
7. Yukie Saitoh, Wang Hongwei, Hiroaki Ueno, Masanari Mizuta, Masamitsu Nakazato. 2010. Candesartan attenuates fatty acid-induced oxidative stress and NAD(P)H oxidase activity in pancreatic #-cells. *Diabetes Research and Clinical Practice* **90**:1, 54-59. [CrossRef]
8. Gisela Drews, Peter Krippeit-Drews, Martina Düfer. 2010. Oxidative stress and beta-cell dysfunction. *Pflügers Archiv - European Journal of Physiology* **460**:4, 703-718. [CrossRef]
9. Ken Uchino, Ridwan Lin, Syed F. Zaidi, Hiroto Kuwabara, Donald Sashin, Nicholas Bircher, Yue-Fang Chang, Maxim D. Hammer, Vivek Reddy, Tudor G. Jovin, Nirav Vora, Mouhammad Jumaa, Lori Massaro, Julia Billigen, Fernando Boada, Howard Yonas, Edwin M. Nemoto. 2010. Increased Cerebral Oxygen Metabolism and Ischemic Stress in Subjects with Metabolic Syndrome-Associated Risk Factors: Preliminary Observations. *Translational Stroke Research* **1**:3, 178-183. [CrossRef]
10. Annette D. de Kloet, Eric G. Krause, Stephen C. Woods. 2010. The renin angiotensin system and the metabolic syndrome. *Physiology & Behavior* **100**:5, 525-534. [CrossRef]
11. Qiaoke Gong, Molly Davis, Galina Chipitsyna, Charles J. Yeo, Hwyda A. Arafat. 2010. Blocking Angiotensin II Type 1 Receptor Triggers Apoptotic Cell Death in Human Pancreatic Cancer Cells. *Pancreas* **39**:5, 581-594. [CrossRef]
12. Eduardo Rial, Leonor Rodríguez-Sánchez, Eunate Gallardo-Vara, Pilar Zaragoza, Eva Moyano, M. Mar González-Barroso. 2010. Lipotoxicity, fatty acid uncoupling and mitochondrial carrier function. *Biochimica et Biophysica Acta (BBA) - Bioenergetics* **1797**:6-7, 800-806. [CrossRef]
13. Y. Saitoh, W. Hongwei, H. Ueno, M. Mizuta, M. Nakazato. 2009. Telmisartan attenuates fatty-acid-induced oxidative stress and NAD(P)H oxidase activity in pancreatic #-cells. *Diabetes & Metabolism* **35**:5, 392-397. [CrossRef]
14. ZHANG-ZHE PENG, GAO-YUN HU, HONG SHEN, LING WANG, WANG-BIN NING, YAN-YUN XIE, NA-SUI WANG, BING-XIN LI, YI-TING TANG, LI-JIAN TAO. 2009. Fluorofenidone attenuates collagen I and transforming growth factor-#1 expression through a nicotinamide adenine dinucleotide phosphate oxidase-dependent way in NRK-52E cells. *Nephrology* **14**:6, 565-572. [CrossRef]
15. Maria Soledad Rosselli, Adriana L. Burgueño, Julieta Carabelli, Mariano Schuman, Carlos J. Pirola, Silvia Sookoian. 2009. Losartan reduces liver expression of plasminogen activator inhibitor-1 (PAI-1) in a high fat-induced rat nonalcoholic fatty liver disease model. *Atherosclerosis* **206**:1, 119-126. [CrossRef]
16. Sang-Hyun Ihm, Jung-Ok Lee, Su-Jin Kim, Ki-Bae Seung, Valérie B. Schini-Kerth, Kyuk Chang, Min-Ho Oak. 2009. Catechin prevents endothelial dysfunction in the prediabetic stage of OLETF rats by reducing vascular NADPH oxidase activity and expression. *Atherosclerosis* **206**:1, 47-53. [CrossRef]
17. Benbo Song, Donalyn Scheuner, David Ron, Subramaniam Pennathur, Randal J. Kaufman. 2008. Chop deletion reduces oxidative stress, improves # cell function, and promotes cell survival in multiple mouse models of diabetes. *Journal of Clinical Investigation* **118**:10, 3378-3389. [CrossRef]
18. J. David Lambeth, Karl-Heinz Krause, Robert A. Clark. 2008. NOX enzymes as novel targets for drug development. *Seminars in Immunopathology* **30**:3, 339-363. [CrossRef]
19. Melvin R. Hayden , James R. Sowers . 2007. Redox Imbalance in Diabetes. *Antioxidants & Redox Signaling* **9**:7, 865-867. [Citation] [Full Text PDF] [Full Text PDF with Links]